Dominant-negative effect of *SCN5A* N-terminal mutations through the interaction of Na$_v$1.5 α-subunits

Jérôme Clatot[1,2], Azza Ziyadeh-Isleem[1,2], Svetlana Maugenre[1,2], Isabelle Denjoy[1,2,3], Haiyan Liu[4], Gilles Dilanian[1,2], Stéphane N. Hatem[1,2], Isabelle Deschênes[4], Alain Coulombe[1,2], Pascale Guicheney[1,2†], and Nathalie Neyroud[1,2*†]

[1]INSERM, UMR_S 956, IFR14, Paris, France; [2]UPMC Univ Paris 06, UMR_S 956, Fondation ICAN, Groupe Hospitalier Pitié-Salpêtrière, Paris, France; [3]Centre de Référence des Maladies Cardiaques Héréditaires, AP-HP, Hôpital Bichat, Paris, France; and [4]Heart and Vascular Research Center, Case Western Reserve University, MetroHealth Campus, Cleveland, OH, USA

Aims	Brugada syndrome (BrS) is an autosomal-inherited cardiac arrhythmia characterized by an ST-segment elevation in the right precordial leads of the electrocardiogram and an increased risk of syncope and sudden death. *SCN5A*, encoding the cardiac sodium channel Na$_v$1.5, is the main gene involved in BrS. Despite the fact that several mutations have been reported in the N-terminus of Na$_v$1.5, the functional role of this region remains unknown. We aimed to characterize two BrS N-terminal mutations, R104W and R121W, a construct where this region was deleted, ΔNter, and a construct where only this region was present, Nter.
Methods and results	Patch-clamp recordings in HEK293 cells demonstrated that R104W, R121W, and ΔNter abolished the sodium current I_{Na}. Moreover, R104W and R121W mutations exerted a strong dominant-negative effect on wild-type (WT) channels. Immunocytochemistry of rat neonatal cardiomyocytes revealed that both mutants were mostly retained in the endoplasmic reticulum and that their co-expression with WT channels led to WT channel retention. Furthermore, co-immunoprecipitation experiments showed that Na$_v$1.5-subunits were interacting with each other, even when mutated, deciphering the mutation dominant-negative effect. Both mutants were mostly degraded by the ubiquitin−proteasome system, while ΔNter was addressed to the membrane, and Nter expression induced a two-fold increase in I_{Na}. In addition, the co-expression of N-terminal mutants with the gating-defective but trafficking-competent R878C-Na$_v$1.5 mutant gave rise to a small I_{Na}.
Conclusion	This study reports for the first time the critical role of the Na$_v$1.5 N-terminal region in channel function and the dominant-negative effect of trafficking-defective channels occurring through α-subunit interaction.
Keywords	Arrhythmia • Brugada syndrome • Na$_v$1.5 • SCN5A • Sodium

1. Introduction

Brugada syndrome (BrS) is an inherited autosomal-dominant cardiac channelopathy with incomplete penetrance. It is characterized by a structurally normal heart with a typical electrocardiographic (ECG) pattern showing an ST-segment elevation in the right precordial leads (V1−V3) and an increased risk of sudden cardiac death by ventricular fibrillation.[1] Mutations in *SCN5A*, the gene encoding the

cardiac voltage-gated sodium channel Na$_v$1.5, have been identified in ~25% of affected individuals[2] and commonly reveal loss-of-function properties reducing the sodium current I_{Na} either by gating abnormalities, trafficking defects, or premature stop codons leading to haploinsufficiency.[3] Na$_v$1.5 constitutes the α-subunit of the cardiac Na$^+$ channel complex, which includes other transmembrane subunits and intracellular partners that participate in its expression and function.[4] Although Na$_v$1.5 subunits are not known to oligomerize, a dominant-

negative effect of a mutation has been previously reported,[5] and the common polymorphism H558R has been shown to partially restore I_{Na} impaired by mutations when expressed on different constructs,[6,7] suggesting a cooperation between α-subunits.

Several mutations have been identified in the N-terminus of $Na_v1.5$ in patients with BrS or long QT syndrome, but their functional consequences on I_{Na} have not been studied *in vitro*, except for two of them. The non-functional R121W mutant was reported in conduction disease, associated with protein degradation, and the R43Q mutation showed a hyperpolarizing shift of the activation under lidocaine.[8,9] The role of the N-terminal region of $Na_v1.5$ on the trafficking, localization, and regulation of channel function remains largely unknown.

In this study, we characterized two $Na_v1.5$ N-terminal mutations: R104W identified in a BrS patient, R121W which was previously reported,[8] a chimeric channel where the N-terminus of $Na_v1.5$ was deleted, ΔNter, and a construct where only the N-terminus of $Na_v1.5$ was present, Nter. Our results suggest that the N-terminal region of $Na_v1.5$ plays a key role in the cardiac sodium channel function and demonstrate a physical interaction between $Na_v1.5$ α-subunits.

2. Methods

2.1 Patient

The proband was diagnosed with BrS on the basis of a spontaneous type-1 pattern on the 12-lead ECG (ST segment elevation ≥ 2 mm in one or more right precordial leads) and family history according to the consensus report.[1] Blood samples were obtained after signed written informed consent for genetic analyses and after approval by the local ethics committee of the Pitié-Salpêtrière Hospital. The study was conducted according to the principles of the Helsinki Declaration.

2.2 *SCN5A* mutation analysis

DNA was extracted from peripheral blood leucocytes according to standard procedures. Screening for mutations in the *SCN5A* gene (GenBank accession number NG_008934.1) was performed by genomic DNA amplification of all exons and splice junctions. PCR products were directly sequenced with the Big Dye Terminator v.3.1 kit (Applied Biosystems) on an ABI PRISM 3730 automatic DNA sequencer (Applied Biosystems). Variants and mutations were identified by the visual inspection of the sequence with Seqscape software (Applied Biosystems).

2.3 *SCN5A* cDNA cloning and mutagenesis

Plasmids pcDNA3.1-SCN5A (no tag) and pcDNA3.1-GFP-SCN5A (N-terminal-GFP) were the gifts of Dr H. Abriel (Bern, Switzerland). Plasmids pGFP-N3-SCN5A (C-terminal-GFP) and pRcCMV-FLAG-SCN5A (N-terminal-FLAG) were the gifts of Dr F. Le Bouffant (Nantes, France) and Dr N. Makita (Nagasaki, Japan), respectively. The plasmid pcDNA3.1-HA-SCN5A (HA-WT) was the gift of Dr P. Mohler (Columbus, OH, USA). The plasmid pGFP-N3-SCN5A-ΔNter (C-terminal-GFP) was generated by removing the first 381 nucleotides of *SCN5A* (127 amino acids), and replacing residue 128 by a methionine. The plasmid pNter-IRES2-mRFP1 was created by cloning the sequence of the first 132 amino acids of $Na_v1.5$ in the pIRES2-mRFP1 vector carrying the red fluorescent protein reporter gene. All plasmids contain the hH1a isoform of *SCN5A*. The plasmid pcDNA3-CD4-KKXX and the anti-CD4-KKXX antibody were the gifts of Dr J. Mérot (Nantes, France). This plasmid has been designed to express CD4 carrying the KKXX motif of ER retention. Mutants R104W, R104K, R121W, and R878C in $Na_v1.5$ were prepared using the QuikChange II XL Site-Directed Mutagenesis Kit (Stratagene) according to the manufacturer's instructions and verified by sequencing.

2.4 HEK293 cell culture and transfection

HEK293 cells were maintained in DMEM supplemented with 10% heat-inactivated foetal calf serum and 1% penicillin/streptomycin. HEK293 cells, which do not express endogenous Na_v channels, were transfected with pcDNA3.1-GFP-SCN5A WT or mutants in 35-mm dish well using JET PEI (Polyplus Transfection, New York, USA) according to the manufacturer's instructions. Cells were transfected with a total of 0.6 µg of plasmid per 35 mm dish, to avoid saturating currents. To mimic the heterozygous state of the BrS patient, cells were co-transfected with 0.3 µg of pcDNA3.1-GFP-SCN5A WT and 0.3 µg of each mutant channel plasmid. A HEK293 cell line stably expressing human $Na_v1.5$ (gift of Dr H. Abriel, Bern, Switzerland) was cultured in the presence of 25 µg/mL of zeocin (Invitrogen).

2.5 Electrophysiological recordings

Patch-clamp recordings were carried out in cells transfected with a total of 0.6 µg of plasmid to avoid saturating currents, in the whole-cell configuration at room temperature ($22 \pm 1°C$) as previously reported.[10] Solutions for patch-clamp recordings are described in the Supplementary material online.

Ionic currents were recorded by the whole-cell patch-clamp technique with the amplifier Axopatch 200B, (Axon Instruments, CA, USA). Patch pipettes (Corning Kovar Sealing code 7052, WPI) had resistances of 1.5–2.5 MΩ. Currents were filtered at 5 kHz (-3 dB, 8-pole low-pass Bessel filter) and digitized at 30 kHz (NI PCI-6251, National Instruments, Austin, TX, USA). Data were acquired and analysed with ELPHY® software (G.Sadoc, CNRS, Gif/Yvette, France).

To measure peak I_{Na} amplitude and determine current–voltage relationships (*I/V* curves), currents were elicited by test potentials of 0.2 Hz frequency to -100 to 60 mV by increments of 5 or 10 mV from a holding potential of -120 mV. For the activation-V_m protocol, currents were elicited by 100-ms depolarizing pulses applied at 0.2 Hz from a holding potential of -120 mV, in 5 or 10 mV increments between -100 and $+60$ mV. The steady-state inactivation-V_m protocol was established from a holding potential of -120 mV and a 2-s conditioning prepulse was applied in 5 or 10 mV increments between -140 and $+30$ mV, followed by a 50-ms test pulse to -20 mV at 0.2 Hz.

Data for the activation-V_m and steady-state availability-V_m relationship of I_{Na} were fitted to the Boltzmann equation:

$$Y = 1/\{ 1 + \exp[-(V_m - V_{1/2})/k]\},$$

where V_m is the membrane potential, $V_{1/2}$ is the half-activation or half-availability potential, and k is the inverse slope factor. For activation-V_m curves, Y represents the relative conductance and k is >0. For availability-V_m curves, Y represents the relative current ($I_{Na}/I_{Na}max$) and k is <0.

2.6 Rat neonatal cardiomyocyte isolation and transfection

All animals were cared according to the *Guide for the Care and Use of Laboratory Animals* (NIH Publication No. 85–23, revised 1996) and under the supervision of authorized researchers in an approved laboratory (agreement number B75-13-08). Neonate 1-day-old rats were euthanized by decapitation. Their hearts were dissected, digested with collagenase A (Roche Diagnostics, Meylan, France) and incubated in culture medium after 1.5 h pre-plating on 60-mm plastic dishes in order to remove fibroblasts. Non-adherent cells were plated at a density of 4×10^5 cells/well on 35-mm dishes containing glass coverslips coated with 10 mg/mL laminin (Roche Diagnostics) in culture medium DMEM (high glucose/ L-glutamine; Gibco ref 41965 039), supplemented with 10% horse serum, 5 FBS, 1% penicillin/streptomycin, cytosine B-D arabinofuranoside 25 mg/mL, and incubated for 24 h ($37°C$, 5% CO_2). Cells were transfected

in a 1%-CO$_2$ incubator with 0.6 µg of N-terminal-GFP fused constructs of WT or mutant Na$_v$1.5 using Lipofectamine 2000 (Invitrogen) according to the manufacturer's instructions.

2.7 Immunocytochemistry

Indirect immunofluorescence was performed on rat neonatal cardiomyocytes (RNC) primary culture fixed with methanol for 10 min at −20°C. Cells were then washed twice for 5 min with phosphate buffer saline (PBS), blocked in PBS-5% BSA for 30 min at room temperature. Cells were incubated for 1 h with primary antibodies: rabbit anti-GFP (1:300, Torrey Pines Biolabs) to detect Na$_v$1.5-GFP, mouse anti-Flag (1:300, Stratagene), chicken anti-calreticulin for ER (1:200, Abcam), rabbit anti-giantin for Golgi apparatus (1:1000, Abcam), rabbit anti-LampI for lysosomes (1:200, Abcam), and rabbit anti-LC3 for proteasome (1:1000, Sigma). Detection was performed after two washes with PBS and 1 h of incubation with secondary antibodies: chicken anti-mouse Alexa Fluor 594, goat anti-rabbit Alexa Fluor 488 (1:1000, Molecular Probes), and the nuclear dye DAPI (1:500, Sigma) diluted in the blocking buffer. Control experiments were performed by omitting the primary antibodies.

2.8 Imaging

Labelled cardiomyocytes were observed with an Olympus epifluorescent microscope (60×). Images were acquired with a CoolSnap camera (Ropper Scientific) and analysed with Metamorph software (Molecular devices) equipped with a 3D-deconvolution module. For each sample, series of consecutive plans were acquired (sectioning step: 0.2 µm).

2.9 Protein extraction

Forty-eight hours after transfection with WT or mutant constructs, HEK293 cells were washed with PBS and lysed in the lysis buffer (50 mM Tris pH 7.5, 500 mM NaCl, 1% NP40, 0.1% SDS, 0.5% deoxycholate, and complete protease inhibitor cocktail from Roche) for 1 h at 4°C on a wheel. The soluble fractions from two subsequent 30 min centrifugations at 14 000 g (4°C) were then used for the experiments. To load each lane of the SDS−PAGE with equivalent amounts of total protein, the protein concentration of each lysate was measured in duplicate by the Bradford assay using a BSA standard curve.

2.10 Biotinylation assay

Forty-eight hours after transfection with WT or mutant constructs, HEK293 cells were washed twice with PBS and biotinylated for 60 min at 4°C using PBS containing 1.5 mg of EZ Link Sulfo-NHS-SS-Biotin (Pierce). Plates were incubated for 10 min at 4°C with PBS-100 mM glycine (to quench unlinked biotin) and washed twice with PBS. Cells were then lysed for 1 h at 4°C with the lysis buffer (composition described in the previous paragraph). After centrifugation at 14 000 g for 30 min (4°C), supernatants were incubated with immobilized neutravidin beads (Pierce) over night at 4°C and pelleted by centrifugation. After three washes with the lysis buffer, the biotinylated proteins were eluted with the Laemmli sample buffer with DTT 2X at 37°C for 30 min. Biotinylated proteins were then analysed by western blot as described below.

2.11 Co-immunoprecipitation

Co-immunoprecipitation experiments were performed as previously described.[11] Briefly, total cell lysates were pre-absorbed with Protein A Dynabeads (Dynal, Norway) for 2 h at 4°C. The unbound extracts were then incubated with Dynabeads Protein A crosslinked to the rat monoclonal anti-HA antibody (clone 3F10, Roche, USA). Western blots were revealed using either the rat monoclonal anti-HA antibody (clone 3F10, Roche, USA) or the mouse monoclonal anti-GFP antibody (Clontech, USA) at 1:1000 dilutions.

2.12 Western blot

Proteins were separated on a 10% acrylamide SDS−PAGE gel, then transferred to a nitrocellulose membrane and incubated with primary antibodies followed by infrared IRDye secondary antibodies (LI-COR Biosciences, USA). Proteins were detected using the Odyssey Infrared Imaging System (LI-COR Biosciences, USA). Signals were quantified using ImageJ software and normalized to WT levels.

2.13 Statistical analysis

Data are presented as means ± SEM. Statistical significance was estimated with SigmaPlot® software by Student's t-test or ANOVA, as appropriate. $P < 0.05$ was considered significant.

3. Results

3.1 Identification of a Na$_v$1.5 N-terminal mutation in a BrS patient

The proband (II.1) was an asymptomatic 33-year-old male with a spontaneous BrS type 1 ECG pattern, combining ST-segment elevation and inverted T waves in lead V1, and an incomplete right bundle branch block pattern (PR = 208 ms, QRS = 124 ms) (*Figure 1A* and *B*). Echocardiography, myocardial scintigraphy, and coronary angiography showed small akinetic areas in the right ventricular infundibulum, healthy coronary arteries, and normal left ventricular function. Programmed electrical stimulation induced sustained ventricular tachycardia degenerating into ventricular fibrillation. The patient received an implantable cardiac defibrillator (ICD). No ICD discharge occurred during the 7-year follow-up. His father presented with similar ECG abnormalities (*Figure 1B*) and died suddenly in his sleep at the age of 61.

SCN5A was screened and a variant, c.310 C > T, was identified in exon 3 in the proband, which induces the substitution of the evolutionarily conserved arginine 104 by a tryptophan (p.R104W) (*Figure 1C−E*). This variant was not found in 300 Caucasian controls and neither in the 14 000 alleles of the NHLBI Exome Sequencing Project (Seattle, WA, http://evs.gs.washington.edu/EVS/); it was not transmitted to the proband's healthy offspring and was considered to be a putative mutation responsible for BrS.

3.2 The R104W mutation abolished I_{Na}

Na$^+$ current was recorded in HEK293 cells 36 h after transfection with WT or R104W constructs. I_{Na} traces and I/V relationships are shown in *Figure 2A* and *B*. Peak current densities and P-values are given in *Table 1*. When the R104W mutant channel was expressed alone, no current could be detected. Conditions known to allow some misfolded proteins to escape the ER quality control and reach their final destination,[12,13] were used such as co-expression of R104W with the Na$_v$β1 subunit, decrease in cell incubation temperature to 30°C and addition of mexiletine (a class I anti-arrhythmic agent), but none of these restored any I_{Na}.

The substitution of arginine 104 by another positively charged residue, lysine, restored only 12% of the WT current, suggesting that the alterations of channel function critically depend on the R104 residue (see Supplementary material online, *Figure S1*). Interestingly, the $V_{1/2}$ of the R104K activation curve was shifted by +8.6 mV, while inactivation was unaffected.
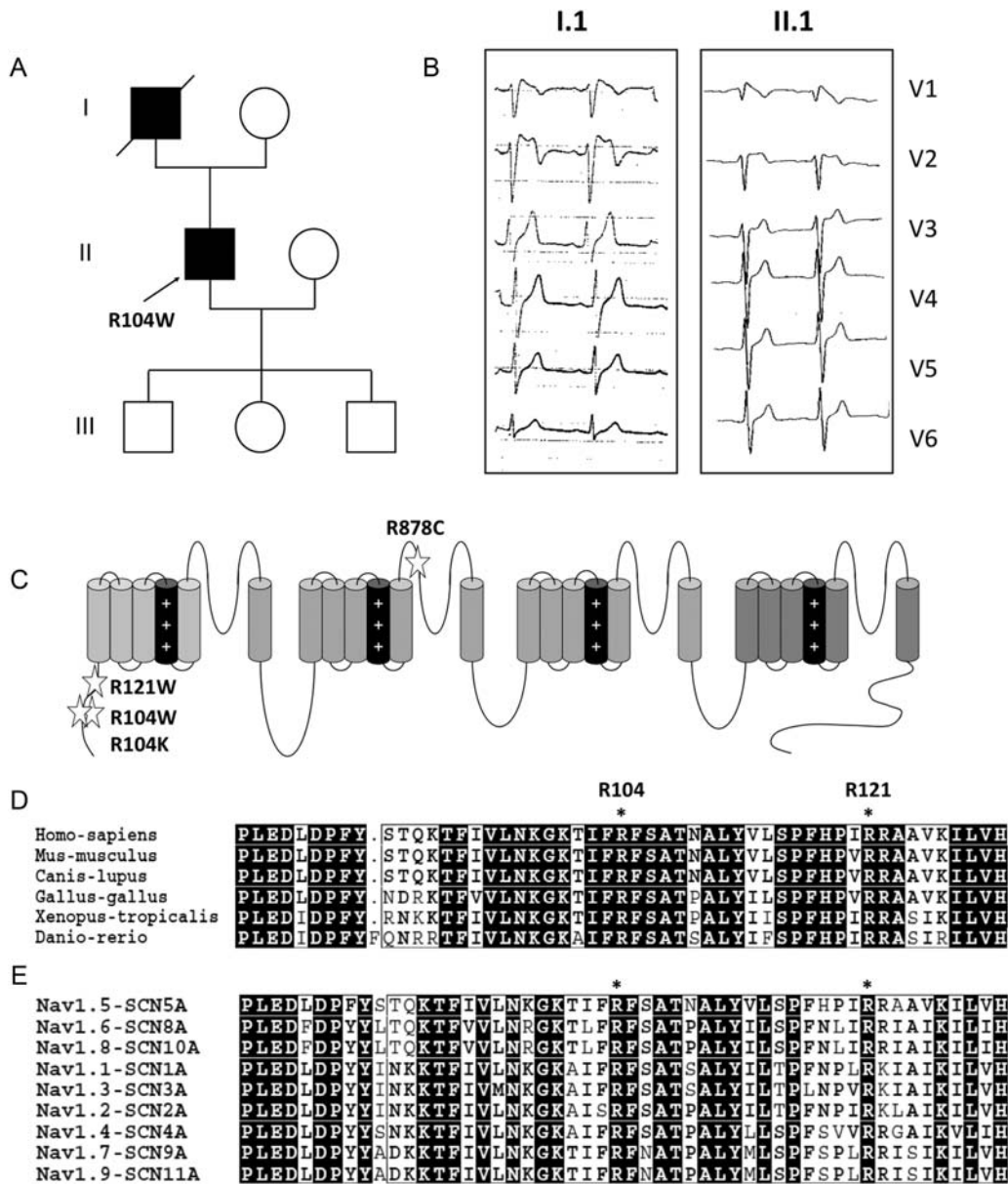
Figure 1 Identification of the R104W *SCN5A* mutation in a patient with BrS. (*A*) Pedigree of the family. The proband (II.1), who carries the mutation, is indicated by an arrow. Squares represent males, circles females, filled symbols affected subjects, and open symbols healthy subjects. (*B*) ECG recordings of precordial leads (V1–V6) of the proband and his father at rest, showing typical type1 BrS pattern. (*C*) Schematic representation of the hNa$_v$1.5 α-subunit. Stars represent the location of mutations characterized in this study. (*D*) Sequences of Na$_v$1.5 N-terminus across species and among voltage-dependent sodium channels (*E*). Conserved amino acids are in boxes. Residues R104 and R121 are indicated by stars. Sequence accession numbers are given in the Supplementary material online.

3.3 Expression in rat neonatal cardiomyocytes

Rat neonatal cardiomyocytes (RNC) transfected with N-terminal-GFP-tagged channel constructs were labelled with an anti-GFP antibody to assess channel location. R104W showed strong perinuclear and intracytoplasmic labelling which was clearly different from WT membrane localization (*Figure 3*). We stained specific sub-cellular compartment proteins, but it is only by cotransfecting RNCs with R104W and CD4 carrying the KKXX motif of ER retention, that we saw an important co-localization of mutant channels and the ER vesicles (*Figure 3*). We compared R104W localization in RNCs to another non-

functional N-terminal Na$_v$1.5 mutant, R121W,[8] and observed that, as R104W, R121W was mostly retained in the ER (*Figure 3*). Interestingly, some WT channels were also retained in intracellular compartments when co-expressed in a 1:1 ratio with R104W (*Figure 4*), suggesting a dominant-negative effect of the N-terminal mutant.

3.4 Dominant-negative effect of N-terminal mutants

To test whether N-terminal mutants had a dominant-negative effect on WT channels, we recorded I_{Na} in HEK293 cells co-transfected with the WT channel and R104W or R121W channel in a 1:1 ratio.
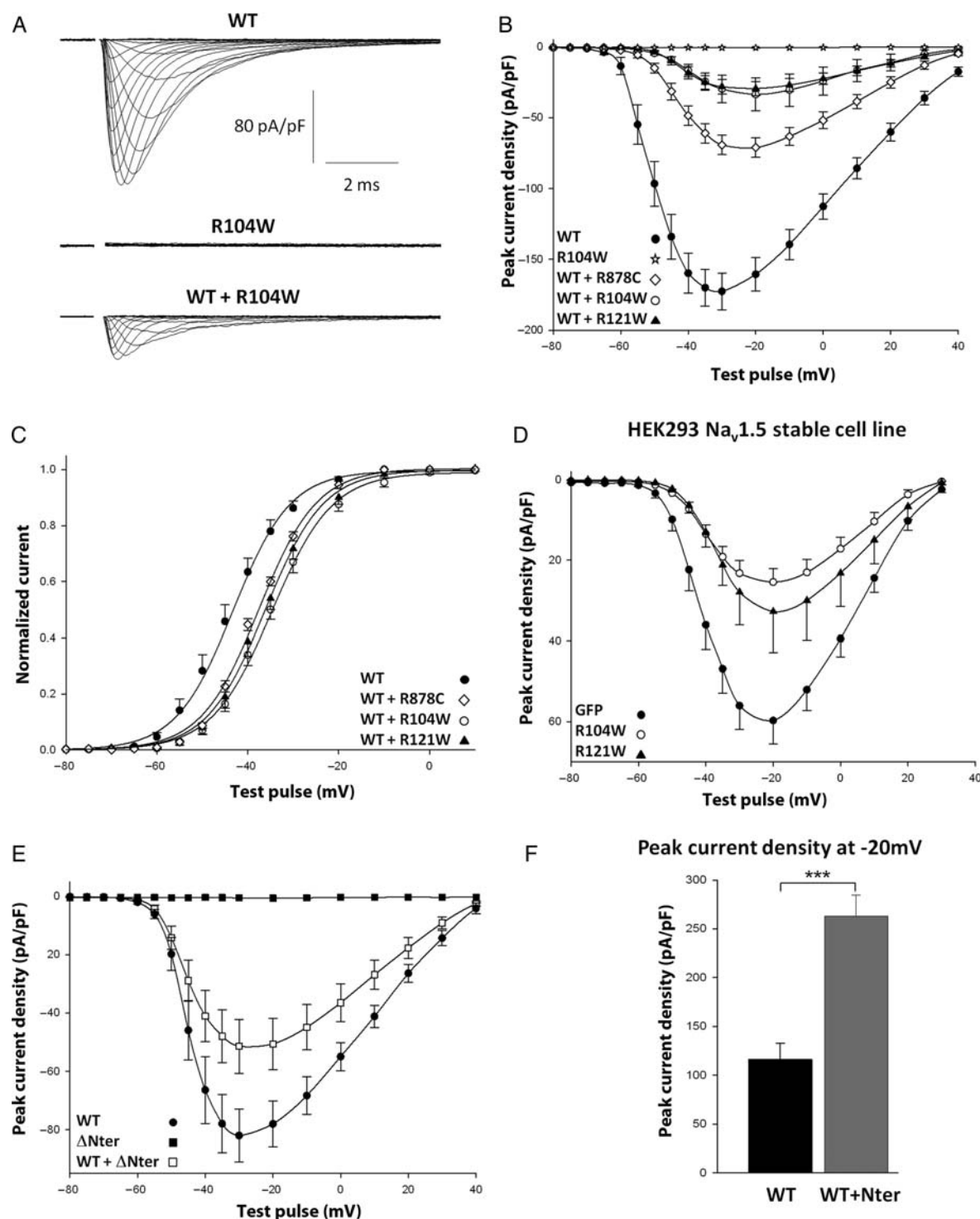
Figure 2 Electrophysiological characterization of Na$_v$1.5 channels. In (A–D) panels, the transfected plasmids carry the N-terminal-GFP-tagged Na$_v$1.5. In (E and F) panels, the GFP is fused to the C-terminus of Na$_v$1.5. Numbers of cells and statistical analysis are indicated in *Table 1*. (A) Representative Na$^+$ current traces of Na$_v$1.5 WT, R104W, and WT+R104W channels. Solid lines indicate the zero current level. (B) Current density–voltage relationships in cells co-transfected with WT, R104W, WT + R104W, WT + R121W, or WT + R878C channels. Only R878C did not exert a dominant-negative suppression on WT I_{Na}. (C) Activation curves of WT + mutants were shifted to more positive potentials (D) Current density–voltage relationships in Na$_v$1.5-stable HEK cells transfected with GFP alone as a control, R104W or R121W mutant channels. Cells were perfused with a 25 mM-Na$^+$ solution to avoid saturating currents. R104W and R121W significantly decreased I_{Na} when compared with cells transfected with GFP alone (GFP: −59.7 ± 5.8 pA/pF, $n = 17$; R104W: −25.5 ± 3.4 pA/pF, $n = 11$, $P = 0.03$; R121W: −32.8 ± 10.1 pA/pF, $n = 7$, $P = 0.03$). (E) Current density–voltage relationships in cells transfected either with WT, ΔNter, or WT + ΔNter. Deletion of the Na$_v$1.5 N-terminus did not exert a dominant-negative effect on WT channels. (F) Peak current density at −20 mV of WT channels alone ($n = 10$) or co-expressed with the N-terminal fragment, Nter ($n = 9$; ***$P<0.001$).

Table I Biophysical and kinetic properties of WT and mutant I_{Na}

GFP position	Na$^+$ channels	Peak current density (pA/pF)	P-value	Activation V$_{1/2}$ (mV)	P-value	k (mV)	P-value	Inactivation V$_{1/2}$ (mV)	P-value	k (mV)	P-value
No GFP	WT	164 ± 27 (n = 8)	ns	−42.7 ± 1.2 (n = 9)	ns	6.4 ± 0.4	ns	−80.1 ± 0.5 (n = 11)	ns	−8.2 ± 0.6	ns
N-term	WT	160 ± 11 (n = 18)		−44.2 ± 1.6 (n = 17)		6.5 ± 0.3		−81.7 ± 0.6 (n = 10)		−8.8 ± 0.5	
	R104W	nd (n = 15)		na		na		na		na	
	R121W	nd (n = 13)		na		na		na		na	
	R878C	nd (n = 15)		na		na		na		na	
	½ WT + ½ R104W	33.6 ± 11.7 (n = 10)	*	−36.5 ± 1.7 (n = 10)	*	6.6 ± 0.2	ns	−82.8 ± 0.5 (n = 9)	ns	−6.6 ± 0.5	**
	½ WT + ½ R121W	29.4 ± 5 (n = 15)	*	−36.8 ± 1.4 (n = 13)	*	6.3 ± 0.2	ns				
	½ WT + ½ R878C	71.1 ± 6.9 (n = 17)	*	−38.3 ± 0.6 (n = 12)	***	6.4 ± 0.2	ns				
	½ R878C + ½ R104W	5.7 ± 1.3 (n = 9)		na		na		na			
	½ R878C + ½ R121W	24.1 ± 4.8 (n = 5)	**	−32.5 ± 1.4 (n = 5)	**	5.8 ± 0.2	ns				
C-term	WT	78.3 ± 7.8 (n = 9)		−43.5 ± 1.1 (n = 9)							
	ΔNter	nd (n = 13)		na							
	½ WT + ½ ΔNter	50.6 ± 8.6 (n = 13)	ns	−41.6 ± 0.9 (n = 10)	ns						

Data are presented as means ± SEM. Peak current density is given at −20 mV.
WT, wild type; nd, not detectable; na, not available because of too small currents; and ns, not significant.
*P ≤ 0.001, **P < 0.05, ***P ≤ 0.005 compared with N- or C-terminal GFP-tagged WT channel. Note that no difference in biochemical parameters was observed between N-terminal-GFP-tagged channel and not tagged Na$_v$1.5.

This led to a drastic reduction in the peak current densities by ∼80% of the WT current density (*Table 1* and *Figure 2B*). In contrast, the co-expression of WT channels and R878C, a trafficking competent but gating-defective mutant[14,15] did not exert a dominant-negative effect, as previously shown[15] (*Table 1* and *Figure 2B*). The N-terminal mutant dominant-negative effect was further confirmed by transfecting a HEK Na$_v$1.5 stable cell line with R104W or R121W (*Figure 2D*).

In cells co-expressing WT and either R104W, R121W, or R878C channels, an unexpected shift of the $V_{1/2}$ of activation to more positive potentials was observed compared with WT alone (*Table 1* and *Figure 2C*). We observed no difference in activation slope factors (*Table 1*). In addition, we observed significant decreases in the fast inactivation time constant of the current and of the fast time constant of recovery from inactivation (see Supplementary material online, *Figure S2*). Voltage-dependent inactivation remained unchanged in cells co-expressing WT and R104W, whereas the slope factor was only slightly increased (*Table 1*).

3.5 Na$_v$1.5 α-subunits interacted with each other

To check whether this dominant-negative effect could be due to an interaction between Na$_v$1.5 α-subunits, we performed co-immunoprecipitation in HEK293 cells transfected with either HA-WT alone, GFP-WT alone, HA-WT + GFP-WT or HA-WT + GFP-R104W (*Figure 5*). Na$_v$1.5 α-subunits tagged with either HA or GFP were used in order to discriminate between the two channels and address whether they interact. When immunoprecipitation was performed with the anti-HA antibody, and western blot revealed with the anti-GFP antibody in cells expressing both HA-WT + GFP-WT or HA-WT + GFP-R104W, a specific band at the expected size was present for both GFP-WT and the GFP-R104W (*Figure 5*, boxed area). This indicates that the HA-WT Na$_v$1.5 α-subunit that was pulled down by the HA antibody, interacted with the GFP-tagged Na$_v$1.5 α-subunit (both, mutant or WT). These results show that an interaction occurs between WT Na$_v$1.5 α-subunits and also between WT and the R104W mutant.

3.6 Deletion of the N-terminus of Na$_v$1.5 abolished I_{Na}

To further characterize the role of the Na$_v$1.5 N-terminal region, we designed a construct where this region was deleted, ΔNter. When expressed alone in HEK293 cells, no current was detected (*Table 1* and *Figure 2E*). In contrast to N-terminal mutants, when ΔNter was co-expressed with WT in a 1:1 ratio, no dominant-negative effect was observed (*Table 1* and *Figure 2E*). In addition, the voltage-dependent activation was unchanged compared with WT, contrasting with the shift observed for co-expression of WT and mutants (*Table 1*).

On the other hand, co-expression of the Na$_v$1.5 N-terminus, Nter, and the full WT channel led to a two-fold increase in I_{Na} density compared with cells expressing WT channels only (*Figure 2F*).

3.7 Degradation of N-terminal mutant channels

Western blots were performed with total transfected HEK293-cell lysates to assess the expression of N-terminal mutants. *Figure 6A* shows a significant decrease in the total protein expression of R104W, R121W, and R104K channels, when compared with WT
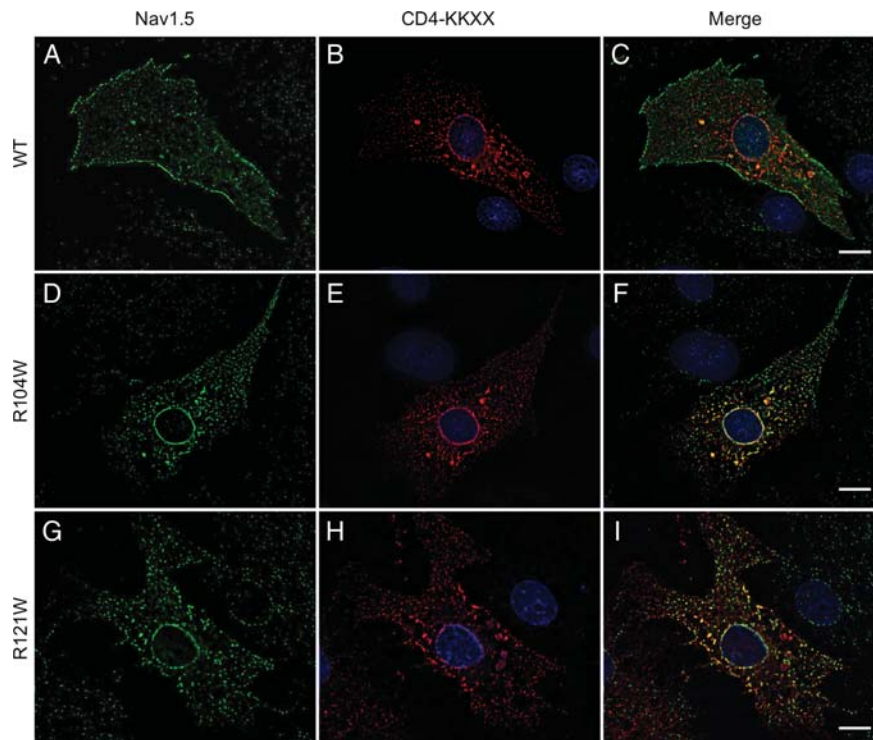
Figure 3 R104W and R121W are mostly retained in the ER in RNC. Three-dimensional deconvolution images of RNC co-transfected with GFP-Na$_v$1.5 (green) and CD4-KKXX (red). Nuclei are stained with DAPI (blue). (*A−C*) Na$_v$1.5 WT, (*D−F*) R104W, and (*G−I*) R121W. Note that in the merged image (*C*) Na$_v$1.5 WT is mostly expressed at the plasma membrane, as opposed to CD4-KKXX, which is retained in the ER. In contrast, N-terminal mutant merged images (*F* and *I*) show numerous internal yellow dots, indicating that Na$_v$1.5 mutants are mostly retained in the ER, similarly to CD4-KKXX. Scale bar: 10 μm.
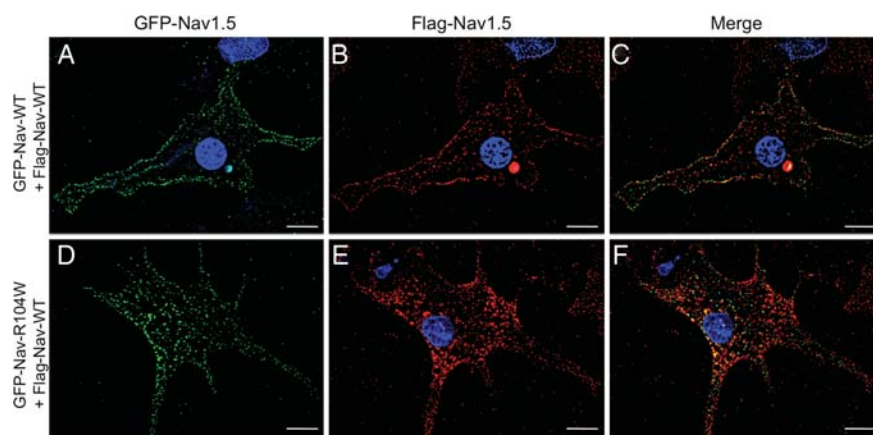

Figure 4 R104W impairs WT channel trafficking in RNC. Three-dimensional deconvolution images of RNCs co-transfected with GFP-Na$_v$1.5 (green) and Flag-Na$_v$1.5 (red). (*A−C*) GFP-Na$_v$1.5-WT + Flag-Na$_v$1.5-WT channels, (*D−F*) GFP-Na$_v$1.5-R104W + Flag-Na$_v$1.5-WT channels. The co-expression of both WT channel constructs exhibits clear membrane staining, whereas the co-expression of WT and R104W mutant shows more intracellular labelling of both channels. Scale bar: 10 μm.

(reduced by 55, 63, and 64%, respectively) or to the R878C mutant. Furthermore, the incubation of cells with the 26S-subunit ubiquitin-proteasome inhibitor, MG132, prevented the degradation of the two N-terminal mutants (*Figure 6B*), without restoring any I_{Na}. To test whether R104W mutant could cause the degradation of WT channels, we co-transfected cells with GFP-tagged and non-tagged channels to distinguish WT from mutant channels. *Figure 6C* shows that WT channels were not degraded in the presence of R104W. To assess whether the N-terminal mutants reached the plasma membrane, we performed cell surface protein biotinylation and showed an important reduction in R104W, R121W, and R104K channel membrane expression compared with WT (reduced by 61, 61, and 91%)
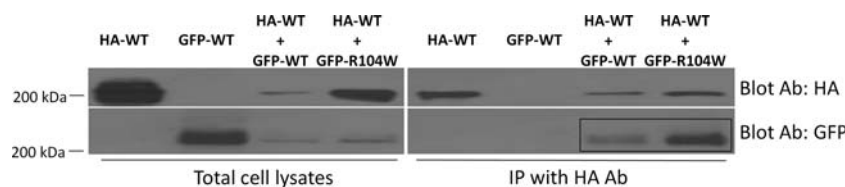
Figure 5 Co-immunoprecipitation of Na$_v$1.5 α-subunits. Co-immunoprecipitation of Na$_v$1.5 α-subunits tagged with either HA or GFP was performed in HEK293 cells. HA-WT, GFP-WT, HA-WT + GFP-WT, or HA-WT + GFP-R104W were transfected as indicated above the lanes. To assess interaction between Na$_v$1.5 α-subunits, the total cell lysates were immunoprecipitated with anti-HA antibody crosslinked to beads. The blots were hybridized with an anti-HA antibody (top gels: blot Ab: HA) or an anti-GFP antibody (bottom gels: blot Ab: GFP). The left side corresponds to the total cell lysates of transfected cells before IP. The right side (IP with HA Ab) corresponds to the elution fractions from beads. The results demonstrated an interaction between Na$_v$1.5 α-subunits, both for WT + WT and WT + mutant (boxed area). These are representative blots from a total of three identical experiments.

or to the R878C mutant (*Figure 6D*). In contrast, ΔNter was slightly degraded (reduced by 21%) but was mostly expressed at the membrane (*Figure 6E*).

Overexpression of N-terminal mutants did not cause reticular stress by the unfolded protein response pathway activation (see Supplementary material online, *Figure S3*).

3.8 Complementation of N-terminal mutants by R878C

In line with the Na$_v$1.5 channel α-subunit cooperation suggested by the dominant-negative effect and the shift of activation, we hypothesized that it might be possible to rescue dominant-negative Na$_v$1.5 mutants by complementation, using the trafficking-competent but non-functional Na$_v$1.5 mutant, R878C. Interestingly, the co-expression of R878C with R104W or R121W in a 1:1 ratio gave rise to small currents of 2 and 8.5% of the WT current, respectively (*Figure 7A and B*). It is noteworthy that the $V_{1/2}$ of activation of the current generated by the co-expression of R121W and R878C was more shifted than the $V_{1/2}$ of activation of the current elicited by the co-expression of R121W and WT (*Table 1* and *Figure 7C*). The activation of R104W + R878C was also likely shifted towards positive potentials, but the activation curve could not be reliably determined because of the too small I_{Na} (*Figure 7B*). Altogether, our results showed the complementation of trafficking-defective and non-functional N-terminal mutants by a non-functional but trafficking-competent Na$_v$1.5 mutant.

4. Discussion

Our study highlights for the first time the important role of the N-terminal domain of Na$_v$1.5. We describe several novel findings by the analysis of two mutant channels, R104W and R121W, and two truncated proteins, ΔNter, and the N-terminus fragment. The two mutants and the truncated channel abolished I_{Na}, but only the mutants exerted a dominant-negative effect on WT channels. Unexpectedly, we demonstrated the capacity of R878C, a trafficking-competent but gating-defective mutant, to partially rescue N-terminal mutant function. Finally, we evidenced an interaction between WT Na$_v$1.5 α-subunits, and we showed that this interaction was still present between WT and R104W channels.

We identified the missense Na$_v$1.5 mutation, R104W, in a young asymptomatic patient with a typical type-1 BrS ECG pattern. The R121W mutation has previously been reported in a BrS patient[2] and in a patient with cardiac conduction disease[8] where it was associated with a loss of channel function and protein degradation. Substitution by a tryptophan of these two conserved arginine abolished I_{Na}, as did the truncation of the N-terminus. Other mutations have also been identified in the Na$_v$1.5 N-terminus in BrS and long QT syndrome patients.[2] Altogether, this suggests the importance of this poorly explored domain in the function of Na$_v$1.5.

In our study, missense mutations in the N-terminus of Na$_v$1.5 led to retention and degradation of most of the channels, while the truncation of the N-terminus did not preclude channels to reach the plasma membrane. The mechanism of mutant channel retention remains to be elucidated. It is likely that cells expressing the mutants use ER-associated degradation (ERAD) as a protective mechanism to remove proteins that fail to acquire their native conformation. Indeed, during ERAD, misfolded proteins are moved from the ER to the cytosol and degraded by the ubiquitin−proteasome system.[16] A similar mechanism has already been highlighted with the N-terminal S21P mutant in Na$_v$1.6, which is retained in the Golgi apparatus and further degraded.[17] Most of the ΔNter channel seemed to escape this quality-control pathway, suggesting that the replacement of arginines 104 and 121 by tryptophans caused severe conformational changes of the N-terminus possibly involved in a negative regulatory pathway.

A dominant-negative effect of mutant ion channel subunits has frequently been reported for channels formed by multiple α-subunits, such as K$_v$LQT1 in long QT syndrome.[18] Na$_v$1.5 α-subunits were not known to interact, therefore, the dominant-negative effect we observed was unexpected, while reported once in studying the trafficking-defective mutation L325R.[5] Here, we highly suggest that the WT cardiac sodium channel α-subunits can interact with each other. Moreover, this interaction, which can be direct or indirect, seems not to be affected by the R104W mutation. This could explain the dominant-negative effect of the missense mutants by an impairment of WT channel trafficking consecutive to the mutant channel retention. Interestingly, several N-terminal mutations in *CACNA1A*, the gene encoding the brain Ca$_v$2.1 channel, whose structure is similar to Na$_v$1.5, induced a dominant-negative effect on WT channels responsible for ataxia,[19,20] leading the authors to postulate
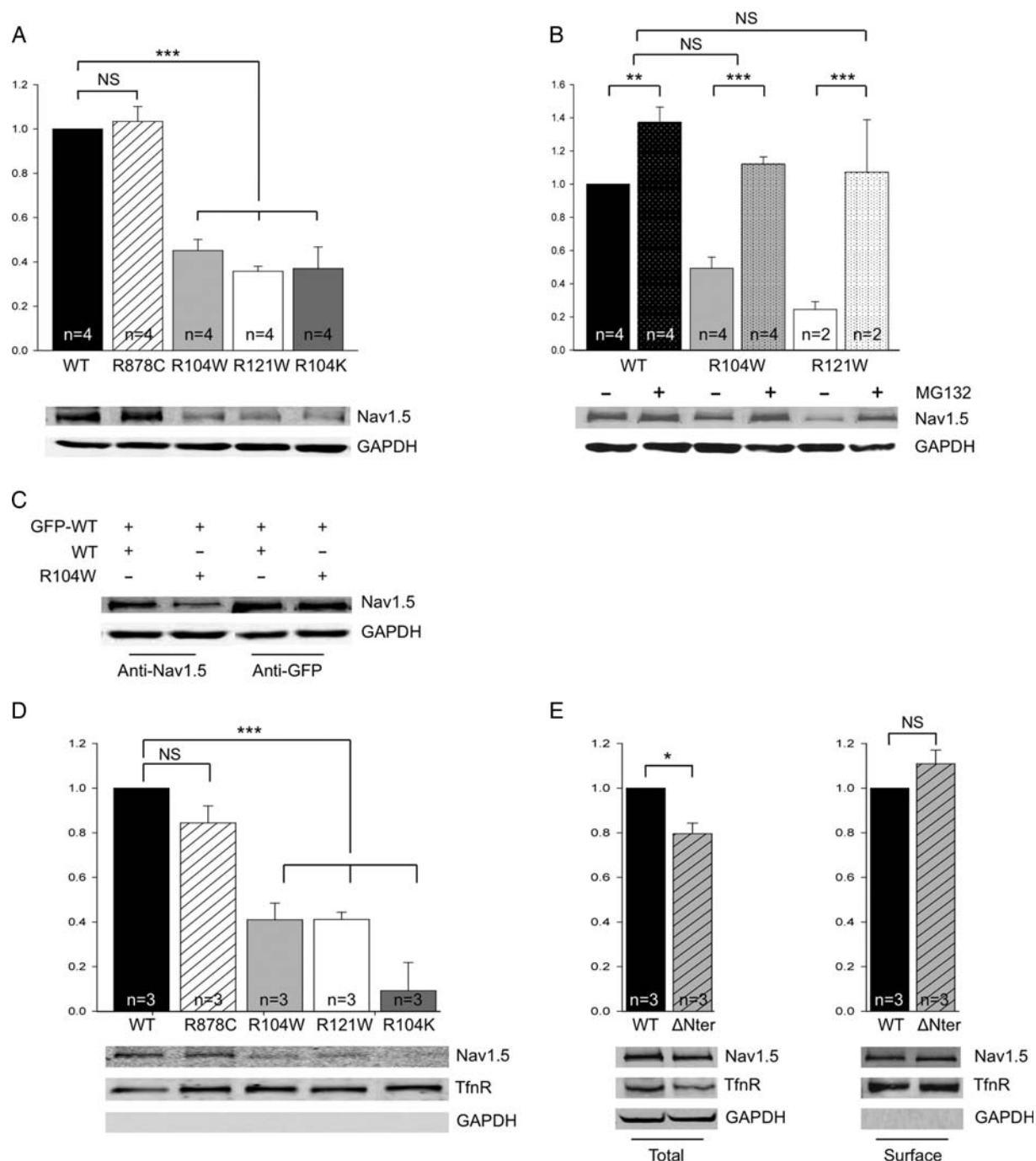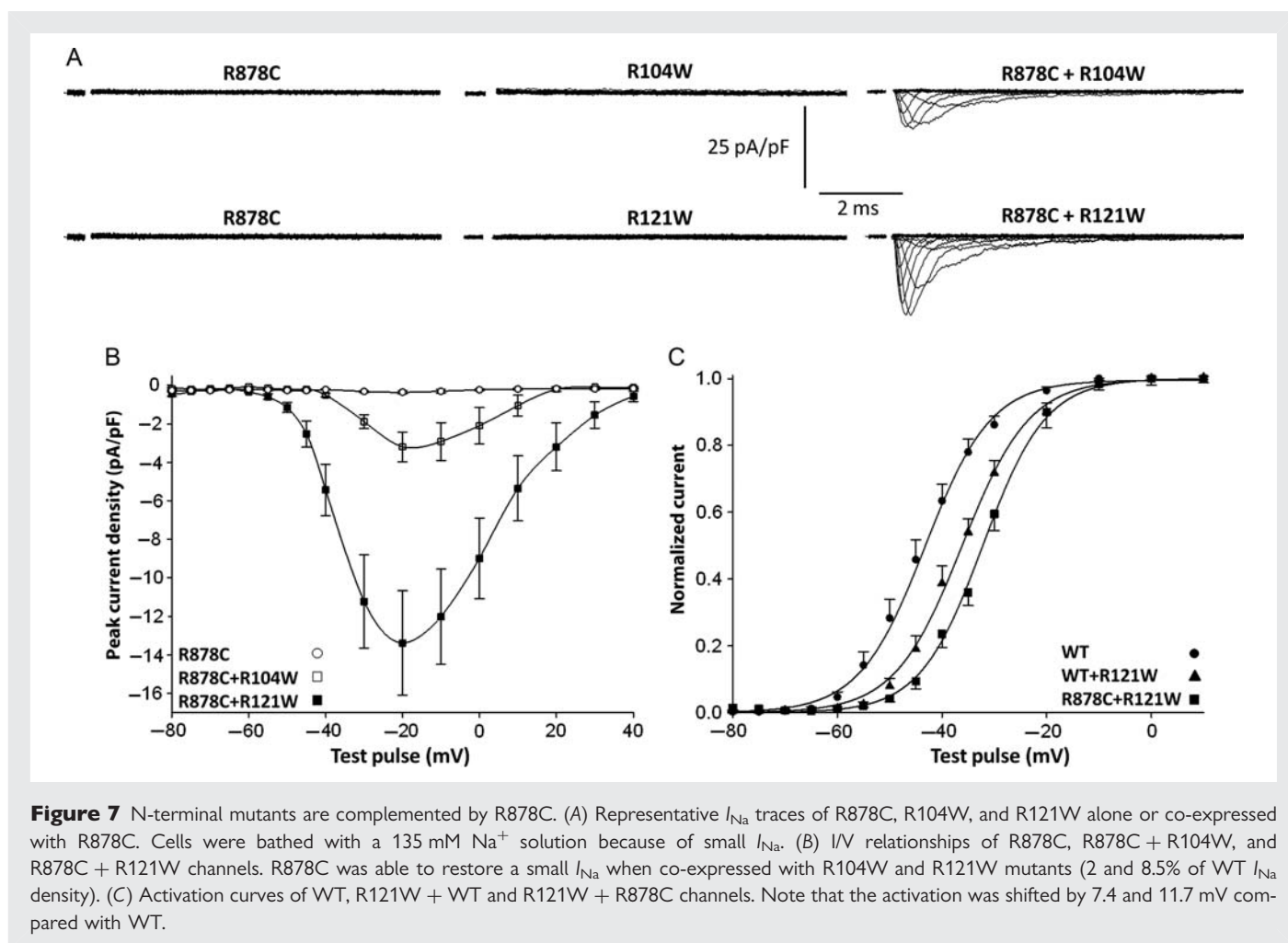
Figure 6 Biochemical analysis. In panels (*A*, *B*, and *D*), cells were transfected with GFP-Na$_v$1.5 and in panel (*E*), with Na$_v$1.5-GFP. NS indicates not significant, **$P = 0.004$ and ***$P \leq 0.001$. Data are represented as arbitrary units. Glyceraldehyde 3-phosphate dehydrogenase (GAPDH) was used as total protein loading control. (*A*) Western blots of total cell lysates show that N-terminal mutant protein quantities are significantly lower than WT (*B*) Incubation of transfected cells with MG132 prevented degradation of N-terminal mutants (*C*) Representative western blot of total protein extracted from cells co-transfected with GFP-Na$_v$1.5 WT and the non-tagged Na$_v$1.5 WT or R104W constructs. The anti-Na$_v$1.5 antibody revealed both channels (tagged and non-tagged) and showed a decrease in the total Na$_v$1.5 channel after cotransfection with the mutant. The anti-GFP antibody revealed only the GFP-Na$_v$1.5-WT channels and showed no degradation of GFP-Na$_v$1.5-WT in the presence of the R104W mutant. (*D*) Cell surface biotinylation experiments. Transferrin receptor (TfnR) was used as a biotinylated protein loading control. Note that the surface membrane expression of N-terminal mutants was markedly reduced compared with WT and R878C. (*E*) Western blot of total cell lysates and biotinylation of cells transfected with ΔNter-GFP. ΔNter was slightly degraded compared with WT, while normally expressed at the membrane.

Figure 7 N-terminal mutants are complemented by R878C. (*A*) Representative I_{Na} traces of R878C, R104W, and R121W alone or co-expressed with R878C. Cells were bathed with a 135 mM Na$^+$ solution because of small I_{Na}. (*B*) I/V relationships of R878C, R878C + R104W, and R878C + R121W channels. R878C was able to restore a small I_{Na} when co-expressed with R104W and R121W mutants (2 and 8.5% of WT I_{Na} density). (*C*) Activation curves of WT, R121W + WT and R121W + R878C channels. Note that the activation was shifted by 7.4 and 11.7 mV compared with WT.

that mutant proteins interfere with either the biosynthesis or the trafficking of WT channels.

These results prompted us to explore the possibility of complementation, a concept studied in the field of CFTR channels.[21–23] Previous reports have demonstrated the rescue of trafficking-defective Na$_v$1.5 mutants by co-expressing the H558R polymorphism in a different construct.[6,7] The mechanisms of this 'complementation phenomenon' remain to be elucidated. We propose that the two N-terminal Na$_v$1.5 mutants studied here are subject to two opposite forces: the first, and the strongest, ensures cell quality control and retains the mutants in the ER impairing WT channel trafficking, whereas the second, through an interaction between α-subunits, drives the mutant channels to the plasma membrane and restores the function of a very small proportion of mutant channels.

Interestingly, our experiments led us to determine the role of the Na$_v$1.5 N-terminus in the function of the channel. Indeed, the co-expression of Nter with the WT channel increased I_{Na} density, suggesting that the presence of the N-terminal fragment enhances WT channel trafficking. This occurs by an unknown mechanism, nevertheless, we can hypothesize that Nter acts as a decoy, allowing more WT channels to bypass a regulatory system and reach the plasma membrane. Moreover, when we truncated the Na$_v$1.5 N-terminus in the ΔNter channel, the channel was correctly addressed to the plasma membrane but was unable to generate any current, suggesting that the N-terminal region is crucial to channel opening.

Furthermore, we showed that R104K induced a small I_{Na} with a positive shift of voltage-dependent activation compared with WT channels. Similarly, co-transfection of the N-terminal mutants with either WT or R878C channels led to a positive shift of voltage-dependent activation. Our results are in accordance with a previous study by Lee *et al.*,[24] who demonstrate that the activation of Na$_v$1.2 and Na$_v$1.6 depends on their respective N-terminal sequence. Besides, these results are in concordance with the significant decreases in the fast inactivation time constant of the current and of the fast time constant of recovery from inactivation that we observed in cells co-expressing WT and R104W channels. To our knowledge, the present study is the first to support that the N-terminal part of Na$_v$1.5 can play a role in the kinetics of the cardiac sodium channel. The mechanism by which the presence of the mutants at the plasma membrane affects the kinetics of WT channels remains to be investigated. Nevertheless, these results are consistent with another study showing a tight cooperation in channel gating by double and triple simultaneous openings, suggesting a mechanism of synergy between Na$_v$ channels.[25] We propose that this synergy occurs by interaction between Na$_v$1.5 α-subunits.

From a clinical point of view, the R104W mutation, heterozygous in the BrS patient, should be associated with reduced expression of WT channels in cardiomyocytes, through a pathophysiological mechanism leading to retention and degradation of mutant proteins. In addition, Na$_v$1.5 channels present at the membrane would open at a more

positive membrane potential threshold and inactivate faster (loss of function), so a greater voltage stimulus is needed to achieve the cell depolarization contributing to slow down the action potential propagation. These are mechanisms known to contribute to the patient's BrS phenotype. Extrapolation of our data to patient management remains nevertheless hazardous since many other factors, still unknown, may occur to modulate the Na$_v$1.5 function. However, it is worth noting that such Na$_v$1.5 mutations associated with a reduced number of channels at the membrane, and causing shifts in activation, may lead to more severe consequences than reported mutations leading to haploinsufficiency.

Supplementary material

Supplementary material is available at *Cardiovascular Research* online.

References

1. Antzelevitch C, Brugada P, Borggrefe M, Brugada J, Brugada R, Corrado D *et al.* Brugada syndrome: report of the second consensus conference: endorsed by the heart rhythm society and the european heart rhythm association. *Circulation* 2005; **111**:659–670.
2. Kapplinger JD, Tester DJ, Alders M, Benito B, Berthet M, Brugada J *et al.* An international compendium of mutations in the SCN5A-encoded cardiac sodium channel in patients referred for Brugada syndrome genetic testing. *Heart Rhythm* 2010;**7**: 33–46.
3. Wilde AA, Brugada R. Phenotypical manifestations of mutations in the genes encoding subunits of the cardiac sodium channel. *Circ Res* 2011;**108**:884–897.
4. Abriel H. Cardiac sodium channel Na(v)1.5 and interacting proteins: Physiology and pathophysiology. *J Mol Cell Cardiol* 2010;**48**:2–11.
5. Keller DI, Rougier JS, Kucera JP, Benammar N, Fressart V, Guicheney P *et al.* Brugada syndrome and fever: Genetic and molecular characterization of patients carrying SCN5A mutations. *Cardiovasc Res* 2005;**67**:510–519.
6. Poelzing S, Forleo C, Samodell M, Dudash L, Sorrentino S, Anaclerio M *et al.* SCN5A polymorphism restores trafficking of a Brugada syndrome mutation on a separate gene. *Circulation* 2006;**114**:368–376.
7. Shinlapawittayatorn K, Du XX, Liu H, Ficker E, Kaufman ES, Deschenes I. A common SCN5A polymorphism modulates the biophysical defects of SCN5A mutations. *Heart Rhythm* 2011;**8**:455–462.
8. Holst AG, Liang B, Jespersen T, Bundgaard H, Haunso S, Svendsen JH *et al.* Sick sinus syndrome, progressive cardiac conduction disease, atrial flutter and ventricular tachycardia caused by a novel SCN5A mutation. *Cardiology* 2010;**115**:311–316.
9. Lin MT, Wu MH, Chang CC, Chiu SN, Theriault O, Huang H *et al.* In utero onset of long QT syndrome with atrioventricular block and spontaneous or lidocaine-induced ventricular tachycardia: compound effects of hERG pore region mutation and SCN5A N-terminus variant. *Heart Rhythm* 2008;**5**:1567–1574.
10. Kattygnarath D, Maugenre S, Neyroud N, Balse E, Ichai C, Denjoy I *et al.* Mog1: a new susceptibility gene for Brugada syndrome. *Circ Cardiovasc Genet* 2011;**4**:261–268.
11. Deschenes I, Armoundas AA, Jones SP, Tomaselli GF. Post-transcriptional gene silencing of KChIP2 and Navbeta1 in neonatal rat cardiac myocytes reveals a functional association between Na and ito currents. *J Mol Cell Cardiol* 2008;**45**:336–346.
12. Ulloa-Aguirre A, Janovick JA, Brothers SP, Conn PM. Pharmacologic rescue of conformationally-defective proteins: Implications for the treatment of human disease. *Traffic* 2004;**5**:821–837.
13. Valdivia CR, Tester DJ, Rok BA, Porter CB, Munger TM, Jahangir A *et al.* A trafficking defective, Brugada syndrome-causing SCN5A mutation rescued by drugs. *Cardiovasc Res* 2004;**62**:53–62.
14. Gui J, Wang T, Jones RP, Trump D, Zimmer T, Lei M. Multiple loss-of-function mechanisms contribute to SCN5A-related familial sick sinus syndrome. *PloS One* 2010;**5**:e10985.
15. Zhang Y, Wang T, Ma A, Zhou X, Gui J, Wan H *et al.* Correlations between clinical and physiological consequences of the novel mutation R878C in a highly conserved pore residue in the cardiac Na$^+$ channel. *Acta Physiol (Oxf)* 2008;**194**:311–323.
16. Brodsky JL, Scott CM. Tipping the delicate balance: defining how proteasome maturation affects the degradation of a substrate for autophagy and endoplasmic reticulum associated degradation (ERAD). *Autophagy* 2007;**3**:623–625.
17. Sharkey LM, Cheng X, Drews V, Buchner DA, Jones JM, Justice MJ *et al.* The ataxia3 mutation in the N-terminal cytoplasmic domain of sodium channel Na(v)1.6 disrupts intracellular trafficking. *J Neurosci* 2009;**29**:2733–2741.
18. Chouabe C, Neyroud N, Guicheney P, Lazdunski M, Romey G, Barhanin J. Properties of KvLQT1 K$^+$ channel mutations in Romano-Ward and Jervell and Lange-Nielsen inherited cardiac arrhythmias. *Embo J* 1997;**16**:5472–5479.
19. Jouvenceau A, Eunson LH, Spauschus A, Ramesh V, Zuberi SM, Kullmann DM *et al.* Human epilepsy associated with dysfunction of the brain P/Q-type calcium channel. *Lancet* 2001;**358**:801–807.
20. Mezghrani A, Monteil A, Watschinger K, Sinnegger-Brauns MJ, Barrere C, Bourinet E *et al.* A destructive interaction mechanism accounts for dominant-negative effects of misfolded mutants of voltage-gated calcium channels. *J Neurosci* 2008;**28**:4501–4511.
21. Cormet-Boyaka E, Jablonsky M, Naren AP, Jackson PL, Muccio DD, Kirk KL. Rescuing cystic fibrosis transmembrane conductance regulator (CFTR)-processing mutants by transcomplementation. *Proc Natl Acad Sci USA* 2004;**101**:8221–8226.
22. Owsianik G, Cao L, Nilius B. Rescue of functional DeltaF508-CFTR channels by co-expression with truncated CFTR constructs in COS-1 cells. *FEBS Lett* 2003;**554**: 173–178.
23. Villmann C, Oertel J, Ma-Hogemeier ZL, Hollmann M, Sprengel R, Becker K *et al.* Functional complementation of Glra1(spd-ot), a glycine receptor subunit mutant, by independently expressed C-terminal domains. *J Neurosci* 2009;**29**:2440–2452.
24. Lee A, Goldin AL. Role of the amino and carboxy termini in isoform-specific sodium channel variation. *J Physiol* 2008;**586**:3917–3926.
25. Undrovinas AI, Fleidervish IA, Makielski JC. Inward sodium current at resting potentials in single cardiac myocytes induced by the ischemic metabolite lysophosphatidylcholine. *Circ Res* 1992;**71**:1231–1241.